




# Hierarchy of emergent cluster states by measurement from symmetry-protected-topological states with large symmetry to a subsystem cat state

Yoshihito Kuno <sup>1,\*</sup>, Takahiro Orito <sup>2,\*</sup> and Ikuo Ichinose <sup>3</sup>

<sup>1</sup>Graduate School of Engineering Science, Akita University, Akita 010-8502, Japan

<sup>2</sup>Institute for Solid State Physics, The University of Tokyo, Kashiwa, Chiba 277-8581, Japan

<sup>3</sup>Department of Applied Physics, Nagoya Institute of Technology, Nagoya 466-8555, Japan



(Received 9 May 2024; revised 3 July 2024; accepted 12 July 2024; published 25 July 2024)

We propose a *measurement-producing hierarchy* emerging among correlated states by sequential subsystem projective measurements. We start from symmetry-protected-topological (SPT) cluster states with a large symmetry and apply sequential subsystem projective measurements to them and find that generalized cluster SPT states with a reduced symmetry appear in the subsystem of the unmeasured sites. That prescription finally produces Greenberger-Horne-Zeilinger states with long-range order in the subsystem composed of periodic unmeasured sites of the original lattice. The symmetry-reduction hierarchical structure from a general large-symmetric SPT cluster state is clearly captured by the measurement update flow in the efficient algorithm of stabilizer formalism. This approach is useful not only for the analytical search for the measured state, but also for numerical simulation with a large system size. We also numerically verify the symmetry-reduction hierarchy by sequential subsystem projective measurements applied to large systems and large-symmetric cluster SPT states.

DOI: [10.1103/PhysRevB.110.014110](https://doi.org/10.1103/PhysRevB.110.014110)

## I. INTRODUCTION

Quantum measurement applied to a quantum many-body state leads to a change of the state, and sometimes the operation induces an exotic nonlocally correlated state due to the backaction of quantum measurement. In this sense, quantum measurement can be regarded as an important tool to operate quantum many-body systems.

Recently, study in the interdisciplinary area of quantum information and condensed matter physics has rapidly progressed [1]. As a recent hot topic, the interplay of measurements and quantum circuits on many-body systems induces many interesting many-body dynamics and leads to interesting nontrivial steady states depending on the setup of the circuits acting on many-body systems. In particular, random unitary circuits attract much attention. The systems exhibit measurement-induced entanglement phase transitions, which are currently being extensively studied [2–23]. As another topic, measurement-only circuits with a suitable choice of measurement operators and suitable application probabilities generate unconventional phases of matter. Through projective measurements without unitary evolution, various interesting many-body steady states emerge such as symmetry-protected-topological (SPT) phases [24–26], topological orders [27–29], and nontrivial thermal and critical phases [30–34].

Furthermore, by preparing an entangled state called the resource state, the application of measurements with suitable spatial patterns to that state produces a specific entangled state in the subsystems of unmeasured sites. This process

can be applied to a quantum computation, which is called measurement-based quantum computation (MBQC) [35–38]. Such a measurement approach to many-body states is applied not only to carry out a quantum computation, but also to efficiently produce interesting states of matter in condensed matter physics. Recently, in that direction of study, the “cat state” with long-range order (LRO), SPTs, topological ordered states, fractons, and non-Abelian topological ordered states have been efficiently prepared by a measurement procedure applied to some proper entangled states [39–43]. Also, an idea of a stochastic quantum circuit model appearing in such a LRO state was proposed in [44]. More recently, a transition to such a “cat state” through measurements has been observed in a real experimental quantum device [45].

From the viewpoint of the current tendency of research explained above, we shall study the measurement-induced state generation in many-body states by using suitable projective measurements. We present an argument on that issue: From an initial generalized cluster SPT state with large symmetry, a sequential measurement to subsystems induces a series of generalized cluster SPT states with a reduced set of symmetries. That is, we see a *measurement-reduction hierarchy*. After subsystem measurements of suitable times, the initial generalized cluster SPT state reaches a cat state [Greenberger-Horne-Zeilinger (GHZ) state] on a subsystem as the final state. This flow of many-body states can be regarded as a generalization of the methods to produce a cat state with LRO, which was recently proposed in [39–42].

Furthermore, we find efficient feedback-unitary operation for arbitrary projective measurements. Due to the introduction of that feedback unitary, we obtain genuine generalized cluster SPT states and a final GHZ state for any patterns of

\*These authors contributed equally to this work.

measurement outcomes. This approach can be regarded as an extension of the method proposed in [42].

As a result, we show a rich hierarchical structure from large-symmetric SPTs by measurements. We expect that this approach can apply to various many-body quantum systems and induce various correlated quantum many-body states. This work gives concrete examples of the above phenomenon, including the numerical verification for the analytical observations.

The rest of this paper is organized as follows. In Sec. II, we explain generalized cluster spin models and their SPT ground states. These states are target states in this work. In Sec. III, before proposing our main argument, we explain the state preparation scheme for general cluster SPT states by employing a recently proposed prescription on a quantum circuit. In Sec. IV, we present our main argument in this work. There, we first explain the most general argument on states emerging as a result of sequential genuine projective measurements in subsystems. Then, we show a few concrete examples by the analytical calculation using the measurement update in the efficient algorithm of the stabilizer simulation. In Sec. V, we explain feedback unitary, which plays an important role for “erasing” the glassy properties of emergent SPTs. That is, the feedback unitary helps us to create clean hierarchical cluster SPTs as well as final GHZ states. In Sec. VI, we show the results of the numerical simulation by using the efficient algorithm of the stabilizer formalism [46,47], and corroborate our argument for large system sizes and large-symmetric cluster initial states. Section VII is devoted to the conclusion.

## II. GENERALIZED CLUSTER MODEL

This work focuses on the evolution of the ground state by local measurements, the Hamiltonian of which is given by the following generalized cluster spin model [48–52]:

$$H_{\text{gc}}(\alpha) = - \sum_{j=0}^{L-1} Z_j \left[ \prod_{\ell=1}^{\alpha-1} X_{j+\ell} \right] Z_{j+\alpha}, \quad (1)$$

where  $Z_j, X_j$  are Pauli operators and  $\alpha$  is an integer larger than 2. Hereafter, we call the above site-label  $j$  the initial site label, as shown in Fig. 1(a). We mostly employ periodic boundary conditions, that is, the system is a ring composed of  $L$  qubits.

The above  $\alpha$ -cluster model has  $\alpha$ -global symmetries generated by the following operators [53]:

$$G_m^{X,\alpha} = \prod_{\ell=0}^{L/\alpha-1} X_{\alpha\ell+m}, \quad (2)$$

where  $m = 0, 1, \dots, \alpha - 1$ . For any even  $\alpha$ , the ground state is the unique gapped SPT state protected by the  $\alpha$ -global  $Z_2$  symmetries,  $(Z_2)^\alpha$ , corresponding to  $G_m^{X,\alpha}$  ( $m=0, 1, \dots, \alpha-1$ ). The most familiar example is the  $\alpha = 2$  case; the ground state of  $H_{\text{gc}}(2)$  is the cluster state protected by  $Z_2 \times Z_2$  symmetry [54].

On the other hand, for any odd  $\alpha$ , the ground state of  $H_{\text{gc}}(\alpha)$  is doubly degenerate as a result of spontaneous symmetry breaking (SSB) [55], where the broken symmetry is the diagonal symmetry generated by  $\prod_{m=0}^{\alpha-1} G_m^{X,\alpha} \equiv P$  corresponding to the parity operator. Then, each state is a

cluster SPT state protected by the  $(Z_2)^{\alpha-1}$  global symmetries that remain under the SSB of the diagonal symmetry [55]. The twofold degenerate odd- $\alpha$  cluster SPT states are to be distinguished by the sign of the parity operator,  $P \equiv \prod_{j=0}^{L-1} X_j$  (an example is given in [25]). For example, for the  $\alpha = 3$  ( $ZXXZ$ ) model, the ground states are two distinct orthogonal states, each of which corresponds to a cluster SPT state protected by a global  $Z_2 \times Z_2$  symmetry [55] generated by  $G_0^{X,3} G_1^{X,3}$  and  $G_1^{X,3} G_2^{X,3}$ . The SSB for each state can be characterized by a correlator of a local order parameter  $Z_j Y_{j+1} Z_{j+2}$  [53]. Here, we comment that this system plays an important role in quantum computation and quantum error-correcting codes [25]. For the specific  $\alpha = 1$  case, the model is simply the Ising model without a transverse field and the ground states are doubly degenerate  $L$ -site GHZ states with distinct parity  $P = \pm 1$ .

## III. STATE PREPARATION FOR GENERALIZED CLUSTER SPT STATES

Before presenting the main findings of this work, we discuss methods of the state preparation for our target generalized  $\alpha$ -cluster SPT states. Readers who are interested only in the main results obtained in this work can skip to Sec. IV.

Generalized  $\alpha$ -cluster SPT states under consideration can be prepared from a simpler state by using the combination of sequential controlled- $Z$  gates (CZ gates), which is sometimes called the cluster entangler [35,40] and is defined by

$$U_{\text{CZ}} \equiv \prod_{j=0}^{L-1} \text{CZ}_{j,j+1}, \quad (3)$$

where  $\text{CZ}_{j,j+1}$  represents the CZ gate for nearest-neighbor sites  $j$  and  $(j+1)$ . More generally, various cluster SPT states are to be generated by the pivot transformation [56]. The pivot transformation by  $h_k^j$  is defined as

$$U_k^p = \exp \left( i \frac{\pi}{4} \sum_j h_k^j \right), \quad (4)$$

where  $h_k^j$  are given by  $h_k^j = Z_j X_{j+1} \cdots X_{j+k-1} Z_{j+k}$  with  $k > 0$ . In general, the pivot transformation induces the following formula, which we shall use in the following analysis:

$$U_{k_0}^p h_j^k U_{k_0}^{p\dagger} = h_{j+k-k_0}^{2k_0-k}. \quad (5)$$

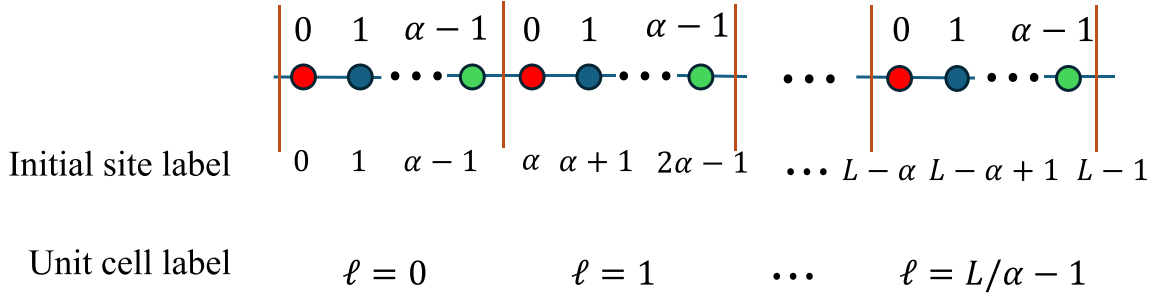
*Even- $\alpha$  case.* We denote a general even- $\alpha$  cluster SPT state as  $|\text{CS}_e(\alpha)\rangle$ , which is the *unique ground state* of the Hamiltonian  $H_{\text{gc}}(\alpha)$ . First, the  $\alpha = 2$  cluster SPT state can be created from the  $+X$  product state (the unique state) denoted by  $|+\rangle^{\otimes L}$  [35,40] as

$$|\text{CS}_e(2)\rangle = U_{\text{CZ}} |+\rangle^{\otimes L}. \quad (6)$$

Based on the state  $|\text{CS}_e(\alpha)\rangle$ , the application of the pivot transformation  $U_{r+2}^p$  to it creates a general  $\alpha = 2r + 2$  ( $r \in \mathbb{N}$ ) even- $\alpha$  cluster SPT state as

$$|\text{CS}_e(\alpha)\rangle = U_{r+2}^p |\text{CS}_e(2)\rangle. \quad (7)$$

## (a) Subsystem label



## (b)

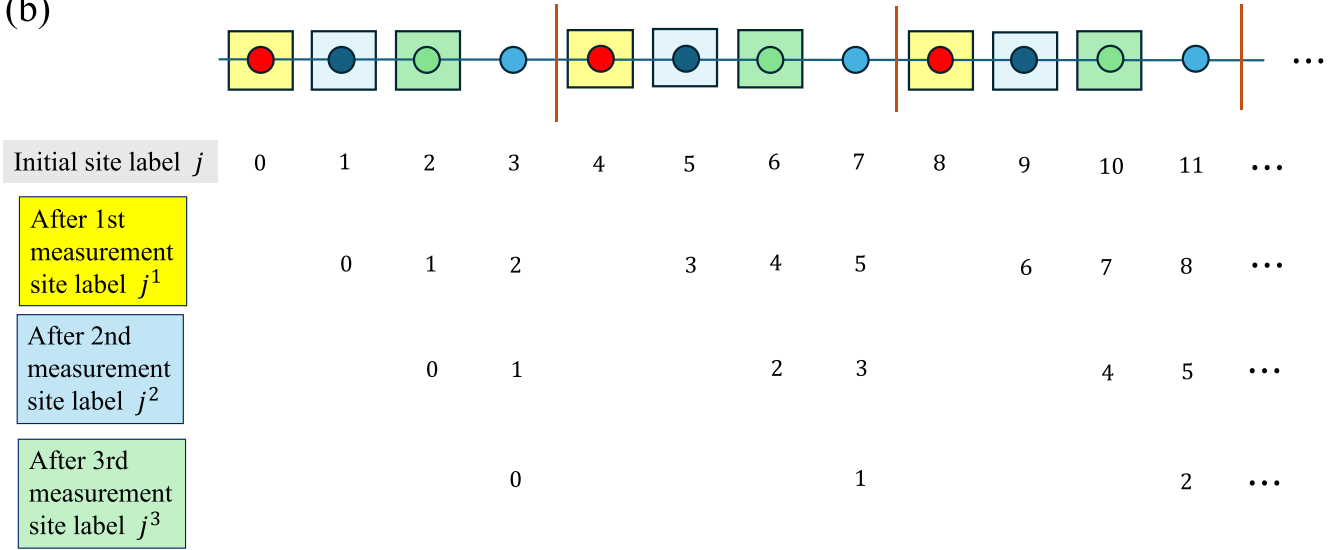


FIG. 1. (a) Setup of the one-dimensional many-qubit system with periodic boundary conditions. One unit cell includes  $\alpha$ -different subsystem sites,  $0, 1, \dots, (\alpha - 1)$ . The red sites are included in the subsystem  $(\text{sys})_0$ , the dark blue ones in the subsystem  $(\text{sys})_1$ , and the green ones in the subsystem  $(\text{sys})_{\alpha-1}$ . The label  $j$  denotes the original site label. The label  $j$  is represented by  $j = \alpha\ell + k$ , where  $\ell$  is the unit cell label and  $k$  is the subsystem label. (b) Rule for labeling site after one measurement step. Here, we show the  $\alpha = 4$  example. Three measurement steps are considered. The unmeasured sites are relabeled in novel consequent order at each measurement step, where the representation is denoted by  $j^{m_s}$  with  $m_s$ . The renumbering of unmeasured sites after a measurement is used for the site definitions of the effective Hamiltonian and stabilizer generators, and the order parameters such as STO and SG. The rule of site labeling is shown in Appendix C.

This comes from the fact that the Hamiltonian  $H_{\text{gc}}(2)$  is transformed by the conjugation of the pivot transformation  $U_{r+2}^p$  as  $U_{r+2}^p H_{\text{gc}}(2) U_{r+2}^{p\dagger} = H_{\text{gc}}(2 + 2r)$ . [Note that  $H_{\text{gc}}(2)$  and  $U_2^p$  commute with each other.] By this transformation, the ground state  $|\text{CS}_e(2)\rangle$  is transformed into  $|\text{CS}_e(2 + 2r)\rangle$ . Please note that the uniqueness of the ground state is preserved in this transformation.

In this way, we can prepare any even- $\alpha$  cluster SPT state from the simple product state.

*Odd- $\alpha$  case.* Next, let us discuss the preparation of a general odd- $\alpha$  cluster SPT state. Note that the ground state is twofold degenerate in this case [53,55]. In this work, we mostly focus on one of the degenerate ground states, i.e., an eigenstate of the parity  $P = \prod_{j=0}^{L-1} X_j$ , which is a logical operator from the quantum information point of view. We start from one of the GHZ ground states of the quantum Ising Hamiltonian  $H_{ZZ} = -\sum_j Z_j Z_{j+1}$ , i.e., the ground state with even parity  $P = +1$  such as  $|\text{GHZ}_+\rangle = \frac{1}{\sqrt{2}}(|\uparrow\rangle^{\otimes L} + |\downarrow\rangle^{\otimes L})$ . From the state  $|\text{GHZ}_+\rangle$ , application of the pivot

transformation  $U_{r+1}^p$  creates a general  $\alpha = 2r + 1$  ( $r \in \mathbb{N}$ ) cluster SPT state as

$$|\text{CS}_o(\alpha)\rangle = U_{r+1}^p |\text{GHZ}_+\rangle. \quad (8)$$

It is straightforward to show that the resultant state  $|\text{CS}_o(\alpha)\rangle$  has positive parity  $P = +1$ .

Here, we remark that the pivot transformation for arbitrary  $k$  can be implemented by a combination of quantum gates on the quantum circuit. Therefore, by using the cluster entangler and the pivot transformation, we can prepare any even- and odd- $\alpha$  cluster SPT states from the two kinds of states  $|\rightarrow\rangle^{\otimes L}$  and  $|\text{GHZ}_+\rangle$ , respectively.

#### IV. SEQUENTIAL SUBSYSTEM MEASUREMENTS FOR A GENERAL CLUSTER SPT STATE

In this section, we shall give a qualitative discussion on states emerging through sequential subsystem measurements starting from cluster SPT states, i.e., the ground states of  $H_{\text{gc}}(\alpha)$  for various  $\alpha$ 's. Then, we show two concrete examples

in small systems by using the analytically tractable update methods in the efficient algorithm of stabilizer formalism. Furthermore, by making use of suitable feedback unitary incorporating information of outcomes [42], we show that the ‘‘hierarchical structure’’ of the resultant states appears for any measurement outcomes. (The details will be discussed in the subsequent section.) There, entanglement, topological properties, and symmetries exhibit interesting behavior under sequential local measurements. This is one of the main findings of this study.

### A. General argument

*General argument for even- $\alpha$  case.* We first consider a general even- $\alpha$  case. The  $\alpha$ -cluster SPT pure state  $|\text{CS}_e(\alpha)\rangle$  is defined on the ring with length  $L = \alpha N$ , where  $L$  is the total number of sites with periodic boundary conditions and  $N$  is the number of unit cells. As shown in Fig. 1(a), the site-label  $j$  is the initial site label,  $j = 0, 1, \dots, L - 1$ , and we introduce  $\alpha$  subsystems, which have  $L/\alpha$  lattice sites. Here, sites in each  $\alpha$  subsystem are numbered as  $(\text{sys})_k = \{j = \alpha\ell + k | \ell = 0, \dots, L/\alpha - 1\}$  for  $k = 0, 1, \dots, \alpha - 1$ , where  $\ell$  numbers unit cells and  $k$  labels internal sites (corresponding to the subsystem label) in a unit cell. These schematics are also shown in Fig. 1(a).

We consider performing a sequence of one-layer projective measurements acting on all sites in the subsystem  $(\text{sys})_k$ . The one-layer projective measurement operator is given by

$$P_{\vec{\beta}^k}^k = \prod_{j \in (\text{sys})_k} \frac{1 + \beta_j X_j}{2}, \quad (9)$$

where  $\vec{\beta}^k = \{\beta_{0+k}, \beta_{\alpha+k}, \dots, \beta_{\alpha(L/\alpha-1)+k}\}$  is a set of measurement outcomes defined on the subsystem  $(\text{sys})_k$  corresponding to the eigenvalue of  $X_j$  with  $\beta_j = \pm 1$ .

We first apply the measurement  $P_{\vec{\beta}^0}^0$ , that is, measure all of the sites of the subsystem  $(\text{sys})_0$ . Here, we regard it as the first measurement step represented by  $m_s = 1$ , where we introduce a label  $m_s$  denoting the number of measurement steps. Then, the initial state changes as follows:

$$P_{\vec{\beta}^0}^0 |\text{CS}_e(\alpha)\rangle \propto |\text{CS}_o^g(\alpha - 1)\rangle \otimes |\vec{\beta}_x^0\rangle_{(\text{sys})_0}. \quad (10)$$

Here,  $|\text{CS}_o^g(\alpha - 1)\rangle$  is a glassy  $(\alpha - 1)$  cluster SPT state with a parity  $P_0 \equiv \prod_{j \in (\text{all}) - (\text{sys})_0} X_j = 1$  through nontrivial correlations between outcomes [See the comments below Eq. (19)], where  $(\text{all}) - (\text{sys})_0$  denotes the set of all sites except the measured sites in  $(\text{sys})_0$  [the label (all) denotes the set of all initial sites, the number of which is  $L$ ]. In addition, the fact that  $P_0 \equiv \prod_{j \in (\text{all}) - (\text{sys})_0} X_j = 1$  gives insight into finding a feedback unitary, discussed in Sec. V. The glassy state  $|\text{CS}_o^g(\alpha - 1)\rangle$  residing on the entire unmeasured sites is one of the twofold degenerate ground states of the effective Hamiltonian given as

$$H^{\text{eff}}(0) = - \sum_{j^1=0}^{L-L/\alpha-1} \beta_{n^0(j^1)} Z_{j^1} \left[ \prod_{\ell=1}^{\alpha-2} X_{j^1+\ell} \right] Z_{j^1+\alpha-1}, \quad (11)$$

where the unmeasured sites after the first step measurement are renumbered in order, and we denote them by  $j^1$ , as explicitly shown in Fig. 1(b), and the labeling rule between

the initial site-label  $j$  and  $j^1$  is given in Appendix C. On the right-hand side of Eq. (11), the site label of outcome  $n^0[j^1]$  denotes the measured site in the support of original operator  $ZX \cdots XZ$  (stabilizer) to which the site  $j^1$  belongs. The labeling rule is given in Appendix C. In terms of the stabilizer formalism [46,57], the representation of the set of the stabilizer generator for the glassy state  $|\text{CS}_o^g(\alpha - 1)\rangle$  is given by  $\mathcal{S}^{\alpha-1} = [g_0^{\alpha-1}, g_1^{\alpha-1}, \dots, g_{L-L/\alpha-1}^{\alpha-1}, P_0]$ , where

$g_{j^1}^{\alpha-1} = \beta_{n^0(j^1)} Z_{j^1} [\prod_{\ell=1}^{\alpha-2} X_{j^1+\ell}] Z_{j^1+\alpha-1}$ . On the other hand, the state  $|\vec{\beta}_x\rangle_{(\text{sys})_0}$  is an  $X$ -directed product state on the subsystem  $(\text{sys})_0$ , where the directions depend on the set of outcomes,  $\vec{\beta}^0$ . Herein, we see that the one-layer projective measurement  $P_{\vec{\beta}^0}^0$  for the  $\alpha$ -cluster SPT state produces the  $(\alpha - 1)$  (odd) cluster SPT state with  $P_0 = +1$  appearing on the unmeasured sites. We also comment that the outcome factors  $\beta$  in the effective Hamiltonian  $H^{\text{eff}}(0)$  can be eliminated by introducing a feedback unitary, as discussed in Sec. V. We can easily expect that by employing the above manipulation in a sequential manner, we obtain a series of glassy cluster SPT states with reduced symmetries defined on the unmeasured sites. That is, as the second step ( $m_s = 2$ ), we further apply another one-layer projective measurement  $P_{\vec{\beta}^1}^1$  to the above state to obtain outcomes  $\vec{\beta}^1 = (\beta_1^1, \beta_{\alpha+1}^1, \dots, \beta_{\alpha(L/\alpha-1)+1}^1)$  on  $(\text{sys})_1$ , and then

$$P_{\vec{\beta}^1}^1 |\text{CS}_o^g(\alpha - 1)\rangle \otimes |\vec{\beta}_x\rangle_{(\text{sys})_0} \propto |\text{CS}_e^g(\alpha - 2)\rangle \otimes |\vec{\beta}_x^0\rangle_{(\text{sys})_0} |\vec{\beta}_x^1\rangle_{(\text{sys})_1}, \quad (12)$$

where  $|\text{CS}_e^g(\alpha - 2)\rangle$  is a glassy  $(\alpha - 2)$  cluster SPT state. The state can be regarded as the unique ground state of the effective Hamiltonian defined on all of the remaining unmeasured sites, given as

$$H^{\text{eff}}(1) = - \sum_{j^2=0}^{L-2L/\alpha-1} \beta_{n^0(j^1[(j^2)^{-1}])} \beta_{n^1(j^2)} Z_{j^2} \left[ \prod_{\ell=1}^{\alpha-3} X_{j^2+\ell} \right] Z_{j^2+\alpha-2}, \quad (13)$$

where the unmeasured sites after the second step measurement are again labeled in order as  $j^2 = j^2[j^1]$ , shown in Fig. 1(b) [its inverse denotes  $j = (j^2)^{-1}$ ], and the label of outcomes  $n^1(j^2)$  is defined as in the previous case (see Appendix C), showing their labeling rules. Here, we see that after the measurement  $P_{\vec{\beta}^1}^1$ , the  $(\alpha - 1)$  cluster SPT state is turned into the  $(\alpha - 2)$  (odd) cluster SPT state appearing on the unmeasured sites. This indicates *reduction hierarchy*: the reduced symmetric glassy cluster SPT state appears on the unmeasured sites. This procedure results in inducing further small symmetric cluster SPT states on the unmeasured sites and, finally, after the  $(\alpha - 1)$ -times one-layer measurements ( $m_s = \alpha - 1$ ) for each subsystem up to  $(\text{sys})_{\alpha-2}$ , the final measured state comes to be

$$\left( \prod_{k=0}^{\alpha-2} P_{\vec{\beta}^k}^k \right) |\text{CS}_e(\alpha)\rangle \propto |\text{GHZ}_+^g\rangle_{(\text{sys})_{\alpha-1}} \bigotimes_{k=0}^{\alpha-2} |\vec{\beta}_x^k\rangle_{(\text{sys})_k}. \quad (14)$$

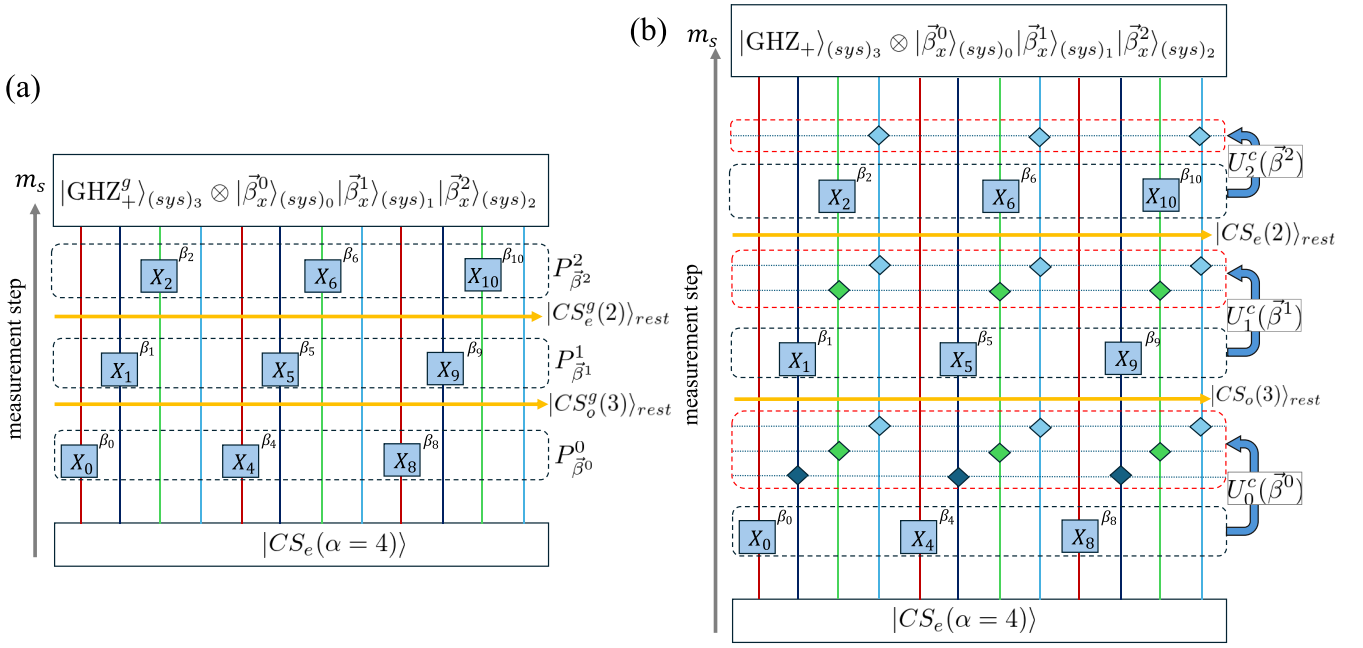


FIG. 2. Schematic circuit picture for the  $\alpha = 4$  and  $N = 3$  cases: (a) Sequential measurements applied to initial  $\alpha = 4$  cluster SPT state. The three different measurement layers on different subsystems are applied. After each measurement step, the reduced cluster SPT states appear on the unmeasured sites and, finally, after  $(\alpha - 1) = 3$  measurement steps, the glassy GHZ state is produced on the unmeasured subsystem  $(\text{sys})_3$ . (b) Measurement and feedback unitary prescription corresponding to LOCC. The red dotted blocks and diamond makers represent feedback unitaries. The line colors in the circuit represent each subsystem, where the red, dark blue, green, and light blue are  $(\text{sys})_0$ ,  $(\text{sys})_1$ ,  $(\text{sys})_2$  and  $(\text{sys})_3$ , respectively. The light-blue lines are the unmeasured sites at the final stage. Here, we observe the clean GHZ state with LRO on the subsystem  $(\text{sys})_3$ .

We see the above  $\alpha$ -period long-range-ordered state as the “glassy GHZ state” with  $P_{\alpha-2} \equiv \prod_{j \in (\text{all}) - \sum_{k=0}^{\alpha-2} (\text{sys})_k} X_j = 1$  denoted by  $|\text{GHZ}_+^g\rangle_{(\text{sys})_{\alpha-1}}$  defined on the subsystem  $(\text{sys})_{\alpha-1}$ . We used the term glassy GHZ state in the above because the orientation of the spin at each unmeasured site varies depending on the outcomes, but there still exists long-range entanglement in the resultant subsystem such as  $\frac{1}{\sqrt{2}}(|\uparrow\uparrow\downarrow\downarrow \dots\rangle + |\downarrow\downarrow\uparrow\uparrow \dots\rangle)$ . The concrete schematic picture of this approach is shown in Fig. 2(a).

*General argument for odd- $\alpha$  case.* Similarly for the general odd- $\alpha$  case, we can apply the same procedure with the even- $\alpha$  case. We start from one of the  $\alpha$ -cluster SPT states with  $P = +1$ , defined on  $L = \alpha N$ , where  $L$  is the total number of sites with periodic boundary conditions and  $N$  is the number of unit cells. Then, we first apply the one-layer projective measurement operator  $P_{\beta_0}^0$  to the initial state ( $m_s = 1$ ). The resultant state is obtained as follows:

$$P_{\beta_0}^0 |CS_o(\alpha)\rangle \propto |CS_e^g(\alpha-1)\rangle \otimes |\vec{\beta}_x^0\rangle_{(\text{sys})_0}, \quad (15)$$

where  $|CS_e^g(\alpha-1)\rangle$  is a glassy  $(\alpha-1)$  (even) cluster SPT state corresponding to the unique ground state of the effective Hamiltonian defined on all of the remaining unmeasured sites,

$$H_e^{\text{eff}}(0) = - \sum_{j^1} \beta_{n^0(j^1)} Z_{j^1} \left[ \prod_{\ell=1}^{\alpha-2} X_{j^1+\ell} \right] Z_{j^1+\alpha-1}, \quad (16)$$

where the unmeasured sites after the first step measurement are again labeled as  $j^1$ , as previously explained in

Fig. 1(b) and Appendix C, and also the label of the outcome factor  $n^0[j^1]$  is defined above.

Then, we apply the second-step projective measurement operator  $P_{\beta_1}^1$  to the former one ( $m_s = 2$ ),

$$P_{\beta_1}^1 |CS_e^g(\alpha-1)\rangle \otimes |\vec{\beta}_x^0\rangle_{(\text{sys})_0} \propto |CS_o^g(\alpha-2)\rangle \otimes |\vec{\beta}_x^0\rangle_{(\text{sys})_0} |\vec{\beta}_x^1\rangle_{(\text{sys})_1}, \quad (17)$$

where  $|CS_o^g(\alpha-2)\rangle$  is a glassy  $(\alpha-2)$  (odd) cluster SPT state with positive parity,  $P_1 = +1$ .

We repeat this prescription. After the  $(\alpha-1)$ -times projective one-layer measurements ( $m_s = \alpha-1$ ), the final state is the same as that of the even- $\alpha$  case,

$$\left( \prod_{k=0}^{\alpha-2} P_{\beta^k}^k \right) |CS_o(\alpha)\rangle \propto |\text{GHZ}_+^g\rangle_{(\text{sys})_{\alpha-1}} \bigotimes_{k=0}^{\alpha-2} |\vec{\beta}_x^k\rangle_{(\text{sys})_k}. \quad (18)$$

Consequently, for any initial  $\alpha$ -cluster SPT state, suitable  $(\alpha-1)$ -layer projective measurements induce  $\alpha$ -period LRO exhibited by the glassy GHZ state.

## B. Concrete example I : $\alpha = 4$ case in a small system

In this section, we examine and verify the above prescription by analytical methods for small-size systems with small  $\alpha$  using the handwritten update procedure of a set of stabilizer generators in the efficient numerical algorithm [46,47]. Readers interested only in the verification of our argument for a large system size and large  $\alpha$  case can skip to Sec. V. The basic transformation of the set of stabilizer generators

and update procedure are explained in Appendices A and B. Observation of the stabilizer generators gives us much insight into the change of the system under projective measurements.

First, as an example of an even- $\alpha$  system, we consider  $L = \alpha N$  with  $N = 3$ . In the stabilizer formalism, the initial  $\alpha = 4$  cluster SPT state is characterized by a set of 12 stabilizer generators denoted by  $\mathcal{S}^{\alpha=4}(m_s = 0)$ , which are given by

$$\mathcal{S}^{\alpha=4}(m_s = 0) = [g_0^4, \dots, g_{11}^4],$$

where  $g_j^4$  is the  $j$ th stabilizer generator given by  $g_j^4 = Z_j X_{j+1} X_{j+2} X_{j+3} Z_{j+4}$  (note that  $j$  is the initial site label).

Let us apply  $P_{\beta_0}^0$ ; then we obtain an updated set of stabilizer generators,

$$\begin{aligned} \mathcal{S}^{\alpha=4}(m_s = 0) &\xrightarrow{P_{\beta_0}^0} \mathcal{S}^{\alpha=4}(m_s = 1) \\ &= [\beta_0 X_0, \beta_4 X_4, \beta_8 X_8, \\ &\quad \beta_4 g_1^3, \beta_4 g_2^3, \beta_4 g_3^3, \beta_8 g_5^3, \beta_8 g_6^3, \beta_8 g_7^3, \\ &\quad \beta_0 g_9^3, \beta_0 g_{10}^3, X_1 X_2 X_3 X_5 X_6 X_7 X_9 X_{10} X_{11}], \end{aligned} \quad (19)$$

where we have used the basic transformation among stabilizer generators several times and re-defined them such as  $g_j^3 = Z_{j^1[j]} X X Z$  and also the last element of the parity  $\prod X$ , both of which are defined on the unmeasured sites. Here, we should remark that the outcomes have the strict correlation  $\beta_8 = \beta_0 \beta_4$ , which stems from the fact that the ground state of the  $\alpha = 4$  Hamiltonian has  $P = +1$ . From the above set of stabilizer generators, the resultant state is obtained as in the form of Eq. (10) with the positive parity.

As the second step, the projective measurement  $P_{\beta_2}^2$  is applied as

$$\begin{aligned} \mathcal{S}^{\alpha=4}(m_s = 1) &\xrightarrow{P_{\beta_1}^1} \mathcal{S}^{\alpha=4}(m_s = 2) \\ &= [\beta_0 X_0, \beta_4 X_4, \beta_8 X_8, \beta_1 X_1, \beta_5 X_5, \beta_9 X_9, \beta_4 \beta_5 g_2^2, \\ &\quad \beta_4 \beta_5 g_3^2, \beta_8 \beta_9 g_6^2, \beta_8 \beta_9 g_7^2, \beta_0 \beta_1 g_{10}^2, \beta_0 \beta_1 g_{11}^2], \end{aligned} \quad (20)$$

where we have made use of the basic transformation for several times,  $g_j^2 = Z_{j^2[j]} X Z$ , and we again find outcome correlations such as  $\beta_9 = \beta_1 \beta_5$ . From this set of the stabilizer generators, we obtain the resultant state as  $|\text{CS}_e^g(2)\rangle \otimes |\vec{\beta}_x^0\rangle_{(\text{sys})_0} \otimes |\vec{\beta}_x^1\rangle_{(\text{sys})_1}$ .

Finally, the last projective measurement  $P_{\beta_2}^2$  is applied as

$$\begin{aligned} \mathcal{S}^{\alpha=4}(m_s = 2) &\xrightarrow{P_{\beta_2}^2} \mathcal{S}^{\alpha=4}(m_s = 3) \\ &= [\beta_0 X_0, \beta_4 X_4, \beta_8 X_8, \beta_1 X_1, \beta_5 X_5, \beta_9 X_9, \\ &\quad \beta_2 X_2, \beta_6 X_6, \beta_{10} X_{10}, \\ &\quad \beta_4 \beta_5 \beta_6 g_3^1, \beta_0 \beta_1 \beta_2 g_{11}^2, X_3 X_7 X_{11}], \end{aligned} \quad (21)$$

with the basic transformation,  $g_j^1 = Z_{j^3[j]} Z$ , and the last element is the parity  $P$  on the subsystem  $(\text{sys})_3$  obtained by the outcomes correlation  $\beta_{10} = \beta_2 \beta_6$ . From this set of stabilizer generators, the stabilizer state corresponds to  $|\text{GHZ}_+^g\rangle_{(\text{sys})_3} \otimes_{k=0}^2 |\vec{\beta}_x^k\rangle_{(\text{sys})_k}$ .

We conclude that we have verified the argument for the  $\alpha = 4$  case in the analytical level by using the update of the efficient algorithm for the stabilizer formalism.

### C. Concrete example II : $\alpha = 3$ case in a small system

Here, as an odd- $\alpha$  example, we consider  $L = \alpha N$  with  $\alpha = N = 3$ . The same calculation as that of the former example can be applied. In fact, the present case is simpler than the former one. In the stabilizer formalism, the  $\alpha = 3$  cluster SPT state with  $P = +1$  is given by an initial set of nine stabilizer generators denoted by  $\mathcal{S}^{\alpha=3}(m_s = 0)$ , given by

$$\mathcal{S}^{\alpha=3}(m_s = 0) = [g_0^3, \dots, g_7^3, X_0 X_1 X_2 X_3 X_4 X_5 X_6 X_7 X_8],$$

where the last element requires that the state is in the  $P = +1$  sector.

Let us apply  $P_{\beta_0}^0$ ; then we obtain the updated set of stabilizer generators,

$$\begin{aligned} \mathcal{S}^{\alpha=3}(m_s = 0) &\xrightarrow{P_{\beta_0}^0} \mathcal{S}^{\alpha=3}(m_s = 1) \\ &= [\beta_0 X_0, \beta_3 X_3, \beta_6 X_6, \beta_3 g_1^2, \beta_3 g_2^2, \beta_6 g_4^2, \beta_6 g_5^2, \beta_0 g_7^2, \beta_0 g_8^2], \end{aligned} \quad (22)$$

where we have used the basic transformation several times and we find the outcomes have the correlation  $\beta_6 = \beta_0 \beta_3$  coming from the positive parity  $P = +1$  of the initial state. From this set of stabilizer generators, the stabilizer state has the form of Eq. (10).

Further, the last projective measurement  $P_{\beta_1}^1$  is applied as

$$\begin{aligned} \mathcal{S}^{\alpha=3}(m_s = 1) &\xrightarrow{P_{\beta_1}^1} \mathcal{S}^{\alpha=3}(m_s = 2) \\ &= [\beta_0 X_0, \beta_3 X_3, \beta_6 X_6, \beta_1 X_1, \beta_4 X_4, \beta_7 X_7, \\ &\quad \beta_3 \beta_4 g_2^1, \beta_0 \beta_1 g_8^1, X_2 X_5 X_8], \end{aligned} \quad (23)$$

with  $g_j^1 = Z_{j^2[j]} Z$ , and the last element is the parity  $P_2$  defined on the subsystem  $(\text{sys})_2$  (We also find the outcomes has the correlation  $\beta_7 = \beta_1 \beta_4$ .) From this set of the stabilizer generators, the stabilizer state corresponds to  $|\text{GHZ}_+^g\rangle_{(\text{sys})_2} \otimes_{k=0}^1 |\vec{\beta}_x^k\rangle_{(\text{sys})_k}$ .

We have verified the argument for the  $\alpha = 3$  case in the analytical level. The case for larger system size and  $\alpha$  is numerically verified in Sec. VI.

## V. INTRODUCING FEEDBACK UNITARY

So far, we have only considered applying the projective measurements  $\{P_{\beta^k}^k\}$  to the subsystem  $(\text{sys})_k$  and focused on the output states depending on random measurement outcomes. In other words, we have mostly observed measurement trajectories. However, recently, a feedback operation with controlled unitary has been proposed in [42], where an initial  $\alpha = 2$  cluster SPT state is turned into a *nonglassy* Ising-type GHZ state on even sites through local measurements on odd sites and feedback operation. Here, we shall give an extension of that feedback unitary for the generic  $\alpha$  systems.

*Feedback unitary for each measurement step.* We discuss the extended feedback at the  $(m_s = k + 1)$ -th measurement step with the outcomes  $\vec{\beta}^k$  denote by  $U_k^f(\vec{\beta}^k)$ , the explicit form of which is given as

$$U_k^f(\vec{\beta}^k) = \prod_{m=k+1}^{\alpha-1} u^m(\vec{\beta}^k), \quad (24)$$

$$u^m(\vec{\beta}^k) = \prod_{\ell=0}^{L/\alpha-1} X_{\alpha\ell+m}^{\frac{1-\prod_{q=0}^{\ell} \beta_{\alpha q+k}}{2}}. \quad (25)$$

Thus, controlled unitary at the  $(m_s = k + 1)$ -th measurement step,  $U_k^c$ , is defined as a composite of the following operators:

$$U_k^c(\vec{\beta}^k) = U_k^f(\vec{\beta}^k)P_{\vec{\beta}^k}^k, \quad (26)$$

$$U_k^c \equiv \sum_{\vec{\beta}^k} U_k^c(\vec{\beta}^k). \quad (27)$$

The form of this controlled unitary  $U_k^c$  can be regarded as an extension of the version proposed in [40,42].

Then, following Ref. [40], we consider sequential measurements with the outcome feedback, starting from a generic even- $\alpha$  cluster SPT state as an example. The first step of the controlled unitary is

$$U_0^c(\vec{\beta}^0)|\text{CS}_e(\alpha) \propto |\text{CS}_o(\alpha - 1)\rangle \otimes |\vec{\beta}_x^0\rangle_{(\text{sys})_0}. \quad (28)$$

On the unmeasured sites, we obtain a *nonglassy*  $(\alpha - 1)$  cluster SPT state denoted by  $|\text{CS}_o(\alpha - 1)\rangle$  with  $P_0 = +1$  corresponding to the positive-parity ground state of the *original Hamiltonian*  $H_{\text{gc}}(\alpha - 1)$  in Eq. (1).

By using this procedure for  $(\alpha - 1)$  times to the initial state, the nonglassy reduced cluster SPT states on the unmeasured sites emerge at each step. By the same procedure explained in Sec. IV A, after  $(m_s = \alpha - 1)$  steps by the controlled feedback  $U_k^c(\vec{\beta}^k)$ , we finally obtain the state in the following form:

$$\left[ \prod_{k=0}^{\alpha-2} U_k^c(\vec{\beta}^k) \right] |\text{CS}_e(\alpha)\rangle \propto |\text{GHZ}_+\rangle_{(\text{sys})_{\alpha-1}} \bigotimes_{k=0}^{\alpha-2} |\vec{\beta}_x^k\rangle_{(\text{sys})_k}. \quad (29)$$

We obtain the  $\alpha$ -period LRO state as the *clean and nonglassy* GHZ state with  $P_{\alpha-2} = +1$  denoted by  $|\text{GHZ}_+\rangle_{(\text{sys})_{\alpha-1}}$  on the subsystem  $(\text{sys})_{\alpha-1}$ . After all,  $(\alpha - 1)$ -times controlled-unitary operations are applied to the  $\alpha$ -cluster SPT state. At each step, we obtain the reduced nonglassy cluster SPT state on the unmeasured subsystem and, finally, get the clean GHZ state, having  $\alpha$ -period LRO. A schematic image of this procedure is shown in Fig. 2(b). Obviously, this manipulation is also applicable for the general odd- $\alpha$  cases.

*Mixed-state picture.* The above procedure is discussed in the purified picture as in Ref. [40]. As proposed in Ref. [42], the manipulation under consideration can be applied to mixed states with the local operation and classical communication (LOCC).

We rewrite the initial state  $|\Psi_0^\alpha\rangle = |\text{CS}(\alpha)\rangle$  in terms of its density matrix  $\rho_0^\alpha = |\Psi_0^\alpha\rangle\langle\Psi_0^\alpha|$ , where we consider one of the twofold degenerate ground states of  $H_{\text{gc}}(\alpha)$  with  $P = +1$  for the odd- $\alpha$  case, and apply the first step ( $m_s = 1$ ) of the controlled unitary  $U_0^c(\vec{\beta}^0)$  to  $\rho_0^\alpha$  [42]; then the density matrix changes as

$$\rho_1^\alpha = \sum_{\vec{\beta}^0} U_0^c(\vec{\beta}^0)\rho_0^\alpha U_0^{c\dagger}(\vec{\beta}^0). \quad (30)$$

The mixed state after the measurement exhibits the order of the  $(\alpha - 1)$  cluster SPT state.

If this approach is repeated  $m_s$  times, we obtain a mixed state after  $m_s$  measurement steps with the feedback, denoted by  $\rho_{m_s}^\alpha$ . The mixed state  $\rho_{m_s}^\alpha$  has the string order of the  $(\alpha - m_s)$  cluster SPT state. We can analytically prove this observation from the finite string order of the  $\alpha$ -cluster SPT state as follows:

$$1 = \langle \text{CS}(\alpha) | \hat{S}(\alpha, \alpha i_0 + m_s, \alpha k_0 + m_s) | \text{CS}(\alpha) \rangle \\ = \text{tr}[\hat{S}(\alpha - m_s, \alpha i_0 + m_s, \alpha k_0 + m_s)\rho_{m_s}^\alpha]. \quad (31)$$

The explicit form of the  $\alpha'$ -string order operator  $\hat{S}(\alpha', \alpha i_0 + m, \alpha k_0 + m)$  is given by Eq. (34) below. The proof of the above equation is given in Appendices D and E.

Finally, we repeat this procedure  $m_s = (\alpha - 1)$  times and obtain the following mixed state density matrix:

$$\rho_{\alpha-1}^\alpha = \sum_{\vec{\beta}^0, \dots, \vec{\beta}^{\alpha-2}} [U_{\alpha-2}^c(\vec{\beta}^{\alpha-2}) \cdots U_0^c(\vec{\beta}^0)] \rho_0^\alpha \\ \times [U_0^{c\dagger}(\vec{\beta}^0) \cdots U_{\alpha-2}^{c\dagger}(\vec{\beta}^{\alpha-2})]. \quad (32)$$

We expect that this density matrix  $\rho_{\alpha-1}^\alpha$  exhibits the following LRO of the Ising GHZ-type such as

$$\text{tr}[\rho_{\alpha-1}^\alpha Z_{i_1} Z_{i_2}] = 1, \quad (33)$$

where  $i_1$  and  $i_2$  are sites of the subsystem  $(\text{sys})_{\alpha-1}$ .

## VI. NUMERICAL VERIFICATION WITHOUT FEEDBACK UNITARY BY USING THE EFFICIENT STABILIZER SIMULATION

We have provided a qualitative discussion and concrete examples of the measurement-reduction hierarchy starting from generalized  $\alpha$ -cluster SPT states. In what follows, we numerically show evidence of the emergent hierarchy structure (for the systems without the feedback unitary), the numerical calculation of which can be performed by using the efficient numerical algorithm for the stabilizer formalism [46,47].

In the numerics, we observe the following quantities. The first one is an extended glassy string order. We expect that the glassy  $\alpha'$ -cluster SPT state can be captured by the following operator [53]:

$$\hat{S}(\alpha', i_0, k_0) = Z_{\alpha' i_0} \left[ \prod_{i=i_0}^{k_0-1} \left( \prod_{m=1}^{\alpha'-1} X_{\alpha' i+m} \right) \right] Z_{\alpha' k_0}. \quad (34)$$

Here, please note that the supports of all the operators reside on the unmeasured sites. The labels are defined by  $j^{m_s}$ , after  $m_s$  measurement steps. As  $\hat{S}(\alpha', i_0, k_0)$  takes positive and negative values randomly reflecting random outcomes, we calculate the squared expectation value of  $\hat{S}(\alpha', i_0, k_0)$  called the glassy string order (STO),

$$S_g(\alpha', i_0, k_0) = |\langle \Psi_s | \hat{S}(\alpha', i_0, k_0) | \Psi_s \rangle|^2, \quad (35)$$

where  $|\Psi_s\rangle$  denotes the SPT states appearing after measurements. This quantity is obtained by checking the commutativity for the stabilizer generators of the state  $|\Psi_s\rangle$  and does not depend on the pattern of the outcomes of measurements; the technical aspect is explained in [26]. When the state  $|\Psi_s\rangle$  is in a (fixed point) glassy  $\alpha'$ -cluster SPT phase,  $S_g(\alpha', i_0, k_0) = 1$  for any  $i_0$  and  $k_0$ . On the other hand, for state  $|\Psi_s\rangle$  not in that phase,  $S_g(\alpha', i_0, k_0) = 0$ .

As the second quantity, we consider the following connected spin-glass long-range order parameter (SGO) [13,29],

$$\text{SG}(i_0, k_0) = |\langle \Psi_s | Z_{i_0} Z_{k_0} | \Psi_s \rangle|^2 - |\langle \Psi_s | Z_{i_0} | \Psi_s \rangle|^2 |\langle \Psi_s | Z_{k_0} | \Psi_s \rangle|^2. \quad (36)$$

Here, note that  $i_0$  and  $k_0$  are both the unmeasured sites, i.e., we are interested in the correlations in the subsystem  $(\text{sys})_{\alpha-1}$ . The SGO characterizes the glassy GHZ phase similar to the spin-glass-ordered phase. The numerical technical aspect is explained in [13]. When the state  $|\Psi_s\rangle$  is a perfect-glassy GHZ state, then  $\text{SG}(i_0, k_0) = 1$  for any  $i_0$  and  $k_0$ . On the other hand, for state  $|\Psi_s\rangle$  not in the GHZ phase,  $\text{SG}(i_0, k_0) = 0$ . The third quantity is the entanglement entropy for a subsystem  $X$  denoted by  $S_X$ . In the stabilizer formalism, the entanglement entropy is related to the number of linearly independent stabilizers in a target subsystem  $X$  [58,59]. It is given by  $S_X = g_X - L_X$ , where  $L_X$  is the system size of the subsystem  $X$ , and  $g_X$  is given by  $\text{rank}|M_X|$ , where the matrix  $M_X$  is obtained by stacking binary-represented vectors of  $L$  stabilizer generators, which are spatially truncated within subsystem  $X$ . In this work, we set  $X$  to a connected half subsystem including  $L/2$  sites of the entire system,  $L_X = L/2$ .

We turn to the numerical setup and results. We prepare  $\alpha = 20$  and  $21$  cluster SPT states as an initial stabilizer state. We apply total  $\alpha - 1$  measurement steps, where we apply the measurement  $P_{\beta^{m_s-1}}^{m_s-1}$  at each measurement step labeled by  $m_s$  ( $m_s = 1, \dots, \alpha - 1$ , where  $m_s = 0$  corresponds to no measurement to the system, that is, the system is in the initial state.) Please note that in the calculation of  $\alpha'$ -STO and SGO at each  $m_s$ , we consider only the unmeasured sites and calculate the  $\alpha'$ -STO and SGO defined on the unmeasured sites labeled by  $j^{m_s}$ , as shown in Fig. 1(b) and Appendix C, that is, no measured sites are included in the definition of the operators. Under this prescription of the site choice, we set  $i_0 = 0$  and  $k_0 = 8$ .

Figure 3 displays results of various  $\alpha'$ -STO and SGO (which is simply the  $\alpha' = 1$  case) along the measurement step  $m_s$ . For the even- $(\alpha = 20)$  case [Fig. 3(a)], we see that at  $m_s = 0$ ,  $S_g(\alpha' = 20, i_0, k_0) = 1$  and the others have zero values. Then, with increasing  $m_s$ , we observe that  $S_g(\alpha' = \alpha - m_s, i_0, k_0) = 1$  and the others have zero value. This indicates that at the measurement step  $m_s$ , a glassy  $\alpha - m_s$  cluster SPT state emerges in the unmeasured subsystems. At the final step  $m_s = \alpha - 1$ , we observe the emergence of a strict glassy GHZ state in the subsystem  $(\text{sys})_{\alpha-1}$  due to  $\text{SG}(i_0, k_0) = 1$ .

For the odd- $(\alpha = 20)$  case [Fig. 3(b)], we observe the same behavior as that of the even- $\alpha$  case. Starting from  $\alpha$ -cluster SPT state, the state reaches the final glassy GHZ state through  $(\alpha - 1)$  sequential measurements by  $P_{\beta^{m_s-1}}^{m_s-1}$ .

These numerical results corroborate the argument in the previous section.

We finally numerically study the entanglement entropy (EE)  $S_{L/2}$ . The results are shown in Fig. 4. For the even- $(\alpha = 20)$  case [Fig. 4(a)], at  $m_s = 0$ , the initial EE is  $S_{L/2} = 20$ , which agrees with the properties of the even- $\alpha$  cluster SPT state [55]. We further observe the linear decreasing behavior of the EE indicating that the  $(\alpha - m_s)$  cluster SPT state is

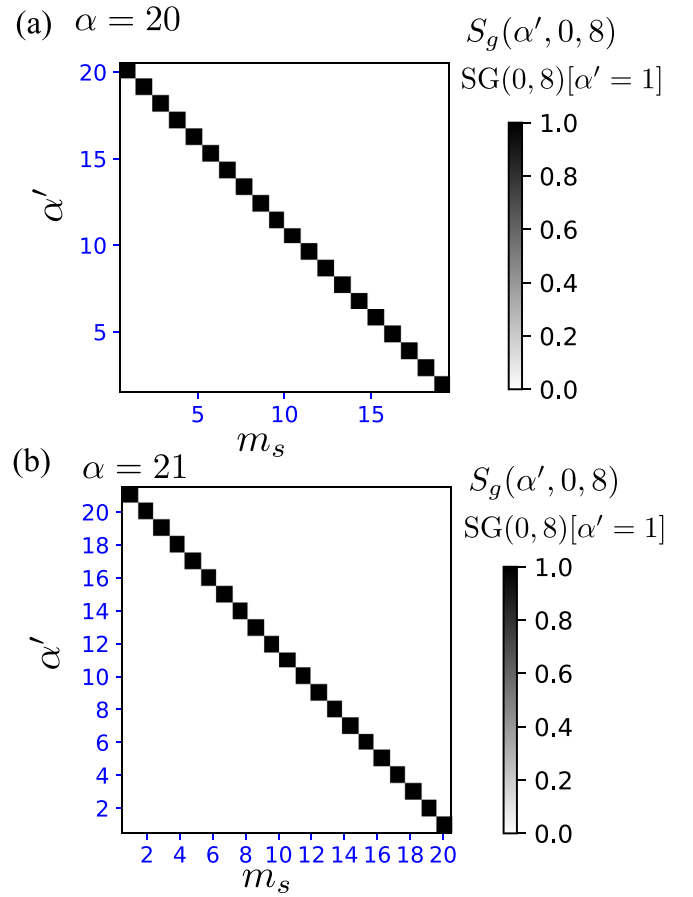


FIG. 3. The values of  $\alpha$ -glassy STO and SGO ( $\alpha' = 1$ ) for (a)  $\alpha = 20$ ,  $N = 20$  and (b)  $\alpha = 21$ ,  $N = 20$ . All order parameters are calculated by employing the relabeled sites defined on the unmeasured sites at each measurement step  $m_s$ .

produced by the measurements. Finally, at  $m_s = \alpha - 1$ , we see  $S_{L/2} = 1$ , indicating the emergence of the glassy GHZ state [29,60].

For the odd- $(\alpha = 21)$  case [Fig. 4(b)], at  $m_s = 0$ , the initial EE is  $S_{L/2} = 21$ , as expected for the odd- $\alpha$  cluster SPT state [55]. We further observe the linear decreasing behavior of the EE similar to that of the even- $\alpha$  case. Finally, at  $m_s = \alpha - 1$ , we also see  $S_{L/2} = 1$ .

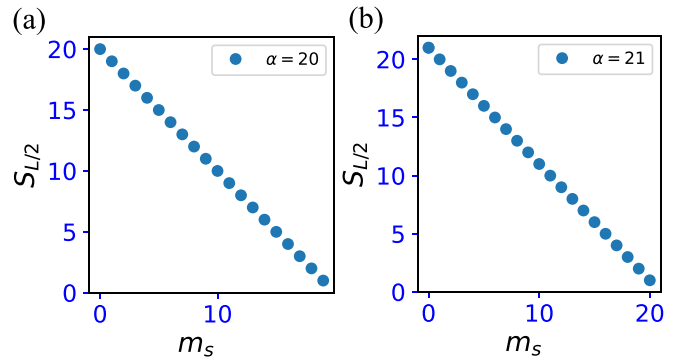


FIG. 4. Half subsystem entanglement entropy  $S_{L/2}$ . (a)  $\alpha = 20$ ,  $N = 20$ , and the total number of the measurement steps is 19. (b)  $\alpha = 21$ ,  $N = 20$ , and the total number of the measurement steps is 20.



Here, we comment that the value of  $S_{L/2}$  is related to the number of emerging edge modes when we introduce a cut of the system or employ open boundary conditions [55]. In addition, the study of the topological response such as the topological pump and edge theory for the generalized cluster model is interesting. Recently, such a direction of study appeared [61]. A study concerning edge modes in the present setup is a future problem.

## VII. CONCLUSION

In this study, we have proposed a measurement-reduction hierarchy of the generalized cluster SPT state by sequential subsystem projective measurements from an initial generalized cluster SPT state with large symmetry. We expect that the sequential subsystem projective measurements induce the series of the glassy cluster SPT states and, finally, a glassy GHZ state. Furthermore, we found efficient feedback unitary regarded as an extension form to that of the previous studies [40,42]. The mixed states created by the sequential controlled unitary exhibit an extended string order at each measurement step, indicating the emergence of the reduced cluster SPT state on the unmeasured sites. The class of the cluster SPT state depends on the number of the measurement step.

We expect that our investigated scheme of sequential measurements for a particular symmetry generator has broad applications to various SPTs defined on high-dimensional systems with a number of large-symmetry groups. There, the reduction procedure can act properly. It has already been shown that at the one-layer level of subsystem measurements, a two-dimensional (2D) cluster SPT turns into a 2D LRO state [40] and a long-range entangled state can be produced [62].

Further, how the bulk measurement affects the topological response and edge theory in the generalized cluster model [61] is also interesting. Such a study has the potential to give a new avenue in this research field.

To apply the findings in this work to practical systems of quantum information, etc., more detailed study of global and topological properties of the extended cluster models is welcome. One interesting and promising direction is a gauging method of the model, which produces a novel and broad class of duality. This prescription has already been applied to the ZXZ model [63]. For the extended cluster models, a couple of similar methods can be considered, which render the global  $Z_2$  symmetries to local ones by introducing “gauge fields.” Using Gauss’s laws, the model Hamiltonian is expressed in terms of gauge-invariant quantities. This is an interesting future work and we hope to report fruitful results on it in the near future.

## ACKNOWLEDGMENTS

This work is supported by JSPS KAKENHI: Grants No. JP23K13026 (Y.K.) and No. JP23KJ0360 (T.O.).

## APPENDIX A: BASIC TRANSFORMATION IN A SET OF STABILIZER GENERATORS

We consider a set of stabilizer generators denoted by  $\{g_0, \dots, g_{N-1}\}$ , where  $N$  generators are included and are

linearly independent of each other. As explained in Ref. [57], there is a standard transformation between stabilizers. We can freely change the set of stabilizer generators by multiplying  $g_i$  by  $g_j$  ( $i \neq j$ ) to obtain a new stabilizer generator  $g_i \rightarrow g_i g_j \equiv g'_i$ . Under this transformation, the stabilizer group obtained from stabilizer generators is invariant. By using this rule including the sign of the stabilizer generators, we can construct a tractable set of stabilizer generators to identify the corresponding many-body states. This prescription works similarly for the stabilizer generators with the outcome factors  $g_i \rightarrow \beta_j g_i$  with  $\beta_j = \pm 1$ . In the standard transformation, we can change the form of the stabilizer generators by multiplying  $\beta_i g_i$  with  $\beta_j g_j$  ( $i \neq j$ ) to obtain a transformed stabilizer generator as  $\beta_i g_i \rightarrow \beta_i \beta_j g_i g_j \equiv \beta_i \beta_j g'_i$ .

## APPENDIX B: UPDATE RULE OF PROJECTIVE MEASUREMENTS IN EFFICIENT NUMERICAL ALGORITHM OF STABILIZER FORMALISM

We review a simple update procedure for a projective measurement in Aaronson-Gottesman efficient stabilizer algorithm [46,47,57]. This update method is efficient not only for numerical calculations, but also for the analytical calculation to deduce a measured many-body state generated by projective measurements with Pauli string measurement operators.

We employ a slightly different notation to include the sign of the outcomes [46,47,57]. This notation is useful to write an effective Hamiltonian after measurements and to elucidate the relations among values of outcomes in distinct sites.

The efficient update way is as follows:

Suppose that a pure state in an  $N$ -qubit system is stabilized by a set of  $N$  stabilizer generators. We denote this set by  $\mathcal{S} = \{g_0, g_1, \dots, g_{N-1}\}$  and call the state under consideration stabilizer state  $\mathcal{S}$ . For this stabilizer state  $\mathcal{S}$ , let us measure the physical quantity corresponding to the operator  $s$  in a Pauli group  $\mathcal{P}_N$  (Pauli string operators), where we consider  $s^2 = 1$  and the outcome takes  $\beta_s = \pm 1$ . (In numerical calculations, we will ignore the sign of the measured value since it does not affect the result for our target physical quantities.)

Then, by the projective measurement on the state  $\mathcal{S}$ , the stabilizer generators are updated as follows [46,47]:

(I) Search anticommutative stabilizer generators to  $s$ . This can be carried out by using the check matrix [57]. From this procedure, as the case 1, we obtain single or some  $m$  anticommutative stabilizer generators,  $g_{\ell_1}, g_{\ell_2}, \dots, g_{\ell_m}$  ( $m \leq N$ ). As the case 2, there is no anticommutative one, and  $\mathcal{S}$  is not updated.

(II) If the case 1 occurs in (I) and there is only a single stabilizer generator denoted by  $g_{m_1}$  that anticommutes to  $s$ , we replace  $g_{m_1}$  with  $\beta_s s$ . Here,  $\beta_s$  is the outcome with probability  $p_{\beta_s} = \sqrt{\langle \Psi_{\text{st}} | P_{\beta_s} | \Psi_{\text{st}} \rangle} = 1/2$  with  $P_{\beta_s} = \frac{1}{2}[I + \beta_s s]$  [57], where  $|\Psi_{\text{st}}\rangle$  is the stabilizer state by  $\mathcal{S}$ . The update of  $\mathcal{S}$  is achieved.

(III) When there are (more than two)  $m$  anticommutative stabilizer generators  $g_{\ell_1}, g_{\ell_2}, \dots, g_{\ell_m}$  ( $m \leq N$ ), replace  $g_{\ell_1}$  with  $\beta_s s$ . Furthermore, for the rest of the anticommutative ones  $g_{\ell_i}$ , update  $g_{\ell_i} \rightarrow g_{\ell_i} g_{\ell_1}$ . By this procedure, the set of

stabilizer generators  $\mathcal{S}$  is updated by the projective measurements with the measurement operator  $s$ .

Furthermore, when we next carry out the projective measurement with a measurement operator  $s'$  with the outcome  $\beta_{s'}$ , we do the above update prescription again, but treat the stabilizer generators with the previous outcome factor  $\beta_s$ , such as  $\beta_s s$ .

### APPENDIX C: RELABEL FUNCTIONS

In this Appendix, we explain the renumbering rule of the unmeasured sites after  $m_s$  measurement steps.

First,  $j$  is the initial site label, as shown in Fig. 1(b). Then, the site relabeling after the first ( $m_s = 1$ ) measurement step is

$$j^1[j] \equiv \left( \left\lfloor \frac{j}{\alpha} \right\rfloor \right) (\alpha - 1) + [(j \bmod \alpha) - 1],$$

for  $j \in (\text{all}) - (\text{sys})_0$ . The site label  $j^1$  labels correctly the unmeasured sites in order, as in Fig. 1(b).

Generally, the site relabeling after  $m_s$  measurement steps denoted as  $j^{m_s}$  is given by

$$j^{m_s}[j] \equiv \left( \left\lfloor \frac{j}{\alpha} \right\rfloor \right) (\alpha - m_s) + [(j \bmod \alpha) - m_s],$$

for  $j \in (\text{all}) - \sum_{k=0}^{m_s-1} (\text{sys})_k$ .

Also, in the effective Hamiltonian, after the first-step measurement, the site label of the outcome factor  $\beta$  is given by

$$n^0[j^1] \equiv \left( \left\lfloor \frac{j^1}{\alpha - 1} \right\rfloor + 1 \right) \alpha + 0.$$

Generally, for the effective Hamiltonian after  $m_s$  measurement steps, the site label of the outcome factor  $\beta$  in the effective Hamiltonian is given by

$$n^{m_s-1}[j^{m_s}] \equiv \left( \left\lfloor \frac{j^{m_s}}{\alpha - m_s} \right\rfloor + 1 \right) \alpha + (m_s - 1).$$

Note that the inverse relabeling function can also be defined for all site-labeling rules appearing here.

### APPENDIX D: PRESENCE OF STRING ORDER AT ANY MEASUREMENT STEP

By extending the observation in [42], we shall prove that a series of the mixed state  $\rho_{m_s}^\alpha$  has its own finite string order.

We start with the  $\alpha$ -cluster SPT state. In the following calculation, we use the initial site label even after any measurements.

The string order for the initial state is

$$\begin{aligned} & \langle \text{CS}(\alpha) | \hat{S}(\alpha, \alpha i_0 + m_s, \alpha k_0 + m_s) | \text{CS}(\alpha) \rangle \\ &= \langle \text{CS}(\alpha) | Z_{\alpha i_0 + m_s} \left[ \prod_{i=i_0}^{k_0-1} (X_{\alpha i+1+m_s} \cdots X_{\alpha i+\alpha-1+m_s}) \right] \\ & \quad \times Z_{\alpha k_0 + m_s} | \text{CS}(\alpha) \rangle = 1. \end{aligned} \quad (\text{D1})$$

Here, we suitably set the sites of the string operators such that the edges of the sites are set as  $\alpha i_0 + m_s$  and  $\alpha k_0 + m_s$ .  $m_s$  is the target number of the measurement steps,  $m_s$ , where we consider  $1 \leq m_s \leq \alpha - 1$ .

The above string order becomes

$$\begin{aligned} & \langle \text{CS}(\alpha) | Z_{\alpha i_0 + m_s} \left[ \prod_{i=i_0}^{k_0-1} (X_{\alpha i+1+m_s} \cdots X_{\alpha i+\alpha-1+m_s}) \right] Z_{\alpha k_0 + m_s} | \text{CS}(\alpha) \rangle \\ &= \sum_{\tilde{\beta}^0, \dots, \tilde{\beta}^{m_s-1}} \langle \text{CS}(\alpha) | [P_{\tilde{\beta}^0}^0 \cdots P_{\tilde{\beta}^{m_s-1}}^{m_s-1}] Z_{\alpha i_0 + m_s} \left[ \prod_{i=i_0}^{k_0-1} (X_{\alpha i+1+m_s} \cdots X_{\alpha i+\alpha-1+m_s}) \right] Z_{\alpha k_0 + m_s} [P_{\tilde{\beta}^{m_s-1}}^{m_s-1} \cdots P_{\tilde{\beta}^0}^0] | \text{CS}(\alpha) \rangle \\ &= \sum_{\tilde{\beta}^0, \dots, \tilde{\beta}^{m_s-1}} \langle \text{CS}(\alpha) | [P_{\tilde{\beta}^0}^0 \cdots P_{\tilde{\beta}^{m_s-1}}^{m_s-1}] Z_{\alpha i_0 + m_s} \left[ \prod_{i=i_0}^{k_0-1} (X_{\alpha i+1+m_s} \cdots X_{\alpha i+\alpha-1}) \right] \left[ \prod_{i=i_0+1}^{k_0} (X_{\alpha i} \cdots X_{\alpha i+m_s-1}) \right] \\ & \quad \times Z_{\alpha k_0 + m_s} [P_{\tilde{\beta}^{m_s-1}}^{m_s-1} \cdots P_{\tilde{\beta}^0}^0] | \text{CS}(\alpha) \rangle \\ &= \sum_{\tilde{\beta}^0, \dots, \tilde{\beta}^{m_s-1}} \langle \text{CS}(\alpha) | [P_{\tilde{\beta}^0}^0 \cdots P_{\tilde{\beta}^{m_s-1}}^{m_s-1}] Z_{\alpha i_0 + m_s} \left[ \prod_{i=i_0}^{k_0-1} (X_{\alpha i+1+m_s} \cdots X_{\alpha i+\alpha-1}) \right] \left[ \prod_{i=i_0+1}^{k_0} (\beta_{\alpha i} \cdots \beta_{\alpha i+m_s-1}) \right] \\ & \quad \times Z_{\alpha k_0 + m_s} [P_{\tilde{\beta}^{m_s-1}}^{m_s-1} \cdots P_{\tilde{\beta}^0}^0] | \text{CS}(\alpha) \rangle \\ &= \sum_{\tilde{\beta}^0, \dots, \tilde{\beta}^{m_s-1}} \langle \text{CS}(\alpha) | \{ P_{\tilde{\beta}^0}^0 \cdots [P_{\tilde{\beta}^{m_s-1}}^{m_s-1} U_{m_s-1}^{f\dagger}(\tilde{\beta}^{m_s-1})] \} Z_{\alpha i_0 + m_s} \left[ \prod_{i=i_0}^{k_0-1} (X_{\alpha i+1+m_s} \cdots X_{\alpha i+\alpha-1}) \right] \left[ \prod_{i=i_0+1}^{k_0} (\beta_{\alpha i} \cdots \beta_{\alpha i+m_s-2}) \right] \\ & \quad \times Z_{\alpha k_0 + m_s} \{ [U_{m_s-1}^f(\tilde{\beta}^{m_s-1}) P_{\tilde{\beta}^{m_s-1}}^{m_s-1}] \cdots P_{\tilde{\beta}^0}^0 \} | \text{CS}(\alpha) \rangle, \end{aligned} \quad (\text{D2})$$

where, in the second line, we have used  $\sum_{\tilde{\beta}^k} P_{\tilde{\beta}^k}^k = \sum_{\tilde{\beta}^k} (P_{\tilde{\beta}^k}^k)^2 = 1$  and, in the last line,

$$U_{m_s-1}^{f\dagger}(\tilde{\beta}^{m_s-1})Z_{\alpha i_0+m_s}(X \cdots X)Z_{\alpha k_0+m_s}U_{m_s-1}^{f\dagger}(\tilde{\beta}^{m_s-1}) = Z_{\alpha i_0+m_s}(X \cdots X) \left[ \prod_{i=i_0+1}^{k_0} \beta_{\alpha i+m_s-1} \right] Z_{\alpha k_0+m_s}. \quad (\text{D3})$$

The proof of this equation is given in Appendix E.

We further proceed with the calculation from Eq. (D2),

$$\begin{aligned} \text{Eq. (2)} &= \sum_{\tilde{\beta}^0, \dots, \tilde{\beta}^{m_s-1}} \langle \text{CS}(\alpha) | \{ [P_{\tilde{\beta}^0}^0 U_0^{f\dagger}(\tilde{\beta}^0)] \cdots [P_{\tilde{\beta}^{m_s-1}}^{m_s-1} U_{m_s-1}^{f\dagger}(\tilde{\beta}^{m_s-1})] \} Z_{\alpha i_0+m_s} \left[ \prod_{i=i_0}^{k_0-1} (X_{\alpha i+1+m_s} \cdots X_{\alpha i+\alpha-1}) \right] \\ &\quad \times Z_{\alpha k_0+m_s} \{ [U_{m_s-1}^f(\tilde{\beta}^{m_s-1}) P_{\tilde{\beta}^{m_s-1}}^{m_s-1}] \cdots [U_0^f(\tilde{\beta}^0) P_{\tilde{\beta}^0}^0] \} | \text{CS}(\alpha) \rangle \\ &= \sum_P \sum_{\tilde{\beta}^0, \dots, \tilde{\beta}^{m_s-1}} \langle \text{CS}(\alpha) | \{ [P_{\tilde{\beta}^0}^0 U_0^{f\dagger}(\tilde{\beta}^0)] \cdots [P_{\tilde{\beta}^{m_s-1}}^{m_s-1} U_{m_s-1}^{f\dagger}(\tilde{\beta}^{m_s-1})] \} | \psi_P \rangle \langle \psi_P | \hat{S}(\alpha - m_s, \alpha i_0 + m_s, \alpha k_0 + m_s) \\ &\quad \times \{ [U_{m_s-1}^f(\tilde{\beta}^{m_s-1}) P_{\tilde{\beta}^{m_s-1}}^{m_s-1}] \cdots [U_0^f(\tilde{\beta}^0) P_{\tilde{\beta}^0}^0] \} | \text{CS}(\alpha) \rangle \\ &= \text{tr}[\hat{S}(\alpha - m_s, \alpha i_0 + m_s, \alpha k_0 + m_s) \rho_{m_s}^\alpha], \end{aligned} \quad (\text{D4})$$

where  $\hat{S}(\alpha - m_s, \alpha i_0 + m_s, \alpha k_0 + m_s)$  is the operator of the  $(\alpha - m_s)$  string order and the sites on the operators are in the unmeasured sites, and  $\rho_{m_s}^\alpha$  is

$$\rho_{m_s}^\alpha = \sum_{\tilde{\beta}^0, \dots, \tilde{\beta}^{m_s-1}} [U_{m_s-1}^c(\tilde{\beta}^{m_s-1}) \cdots U_0^c(\tilde{\beta}^0)] | \text{CS}(\alpha) \rangle \langle \text{CS}(\alpha) | [U_0^{c\dagger}(\tilde{\beta}^0) \cdots U_{m_s-1}^{c\dagger}(\tilde{\beta}^{m_s-1})]. \quad (\text{D5})$$

We have used the completeness relation for a set of  $L$ -site qubit orthogonal basis,  $\sum_P |\psi_P\rangle \langle \psi_P| = 1$ .

From this calculation, from the presence of the string order of the initial  $\alpha$ -cluster SPT state, we conclude that the measured state with feedback after  $m_s$  times one-layer measurements for each different subsystem  $(\text{sys})_k$  for  $k = 0, \dots, m_s - 1$  also has  $(\alpha - m_s)$  string order,

$$1 = \langle \text{CS}(\alpha) | \hat{S}(\alpha, \alpha i_0 + m_s, \alpha k_0 + m_s) | \text{CS}(\alpha) \rangle = \text{tr}[\hat{S}(\alpha - m_s, \alpha i_0 + m_s, \alpha k_0 + m_s) \rho_{m_s}^\alpha]. \quad (\text{D6})$$

From this relation, we expect the presence of the string order for any measurement step except for the  $(\alpha - 1)$  step. This indicates that the cluster SPT state on unmeasured sites exists for any measurement step except for the  $(\alpha - 1)$  step and the class of the string order depends on the numbers of the measurement step  $m_s$ . This relation simply indicates a measurement-reduction hierarchy. Also, Eq. (42) for the  $m_s = \alpha - 1$  case is satisfied, corresponding to the Ising GHZ LRO.

#### APPENDIX E: PROOF OF EQ. (D3)

Here we show the proof of Eq. (D3):

$$\begin{aligned} &U_{m_s-1}^f(\tilde{\beta}^{m_s-1})Z_{\alpha i_0+m_s}(X \cdots X)Z_{\alpha k_0+m_s}U_{m_s-1}^{f\dagger}(\tilde{\beta}^{m_s-1}) \\ &= U_{m_s-1}^f(\tilde{\beta}^{m_s-1})Z_{\alpha i_0+m_s}U_{m_s-1}^{f\dagger}(\tilde{\beta}^{m_s-1})(X \cdots X)U_{m_s-1}^f(\tilde{\beta}^{m_s-1})Z_{\alpha k_0+m_s}U_{m_s-1}^{f\dagger}(\tilde{\beta}^{m_s-1}). \end{aligned} \quad (\text{E1})$$

Here,

$$\begin{aligned} &U_{m_s-1}^f(\tilde{\beta}^{m_s-1})Z_{\alpha i_0+m_s}U_{m_s-1}^{f\dagger}(\tilde{\beta}^{m_s-1}) = u^{m_s}(\tilde{\beta}^{m_s-1})Z_{\alpha i_0+m_s}u^{m_s\dagger}(\tilde{\beta}^{m_s-1}) \\ &= \left( X_{\alpha i_0+m_s}^{\frac{1-\prod_{q=0}^{i_0} \beta_{\alpha q+(m_s-1)}}{2}} \right) Z_{\alpha i_0+m_s} \left( X_{\alpha i_0+m_s}^{\frac{1-\prod_{q=0}^{i_0} \beta_{\alpha q+(m_s-1)}}{2}} \right) = \left[ \prod_{q=0}^{i_0} \beta_{\alpha q+(m_s-1)} \right] Z_{\alpha i_0+m_s}, \\ &U_{m_s-1}^f(\tilde{\beta}^{m_s-1})Z_{\alpha k_0+m_s}U_{m_s-1}^{f\dagger}(\tilde{\beta}^{m_s-1}) = \left[ \prod_{q=0}^{k_0} \beta_{\alpha q+(m_s-1)} \right] Z_{\alpha k_0+m_s}. \end{aligned} \quad (\text{E2})$$

Thus, by substituting the above equations into Eq. (E1), we obtain

$$\text{Eq. (1)} = \left[ \prod_{q=0}^{i_0} \beta_{\alpha q+(m_s-1)} \right] Z_{\alpha i_0+m_s}(X \cdots X) \left[ \prod_{q=0}^{k_0} \beta_{\alpha q+(m_s-1)} \right] Z_{\alpha k_0+m_s} = Z_{\alpha i_0+m_s}(X \cdots X) \left[ \prod_{i=i_0+1}^{k_0} \beta_{\alpha i+m_s-1} \right] Z_{\alpha k_0+m_s}. \quad (\text{E3})$$

- [1] B. Zeng, X. Chen, D.-L. Zhou, and X.-G. Wen, *Quantum Information Meets Quantum Matter: From Quantum Entanglement to Topological Phases of Many-Body Systems* (Springer, New York, 2019).
- [2] Y. Li, X. Chen, and M. P. A. Fisher, *Phys. Rev. B* **98**, 205136 (2018).
- [3] B. Skinner, J. Ruhman, and A. Nahum, *Phys. Rev. X* **9**, 031009 (2019).
- [4] Y. Li, X. Chen, and M. P. A. Fisher, *Phys. Rev. B* **100**, 134306 (2019).
- [5] R. Vasseur, A. C. Potter, Y.-Z. You, and A. W. W. Ludwig, *Phys. Rev. B* **100**, 134203 (2019).
- [6] A. Chan, R. M. Nandkishore, M. Pretko, and G. Smith, *Phys. Rev. B* **99**, 224307 (2019).
- [7] M. Szyniszewski, A. Romito, and H. Schomerus, *Phys. Rev. B* **100**, 064204 (2019).
- [8] S. Choi, Y. Bao, X.-L. Qi, and E. Altman, *Phys. Rev. Lett.* **125**, 030505 (2020).
- [9] Y. Bao, S. Choi, and E. Altman, *Phys. Rev. B* **101**, 104301 (2020).
- [10] C.-M. Jian, Y.-Z. You, R. Vasseur, and A. W. W. Ludwig, *Phys. Rev. B* **101**, 104302 (2020).
- [11] M. J. Gullans and D. A. Huse, *Phys. Rev. X* **10**, 041020 (2020).
- [12] A. Zabalo, M. J. Gullans, J. H. Wilson, S. Gopalakrishnan, D. A. Huse, and J. H. Pixley, *Phys. Rev. B* **101**, 060301(R) (2020).
- [13] S. Sang and T. H. Hsieh, *Phys. Rev. Res.* **3**, 023200 (2021).
- [14] S. Sang, Y. Li, T. Zhou, X. Chen, T. H. Hsieh, and M. P. A. Fisher, *PRX Quantum* **2**, 030313 (2021).
- [15] A. Nahum, S. Roy, B. Skinner, and J. Ruhman, *PRX Quantum* **2**, 010352 (2021).
- [16] S. Sharma, X. Turkeshi, R. Fazio, and M. Dalmonte, *SciPost Phys. Core* **5**, 023 (2022).
- [17] M. P. A. Fisher, V. Khemani, A. Nahum, and S. Vijay, *Annu. Rev. Condens. Matter Phys.* **14**, 335 (2023).
- [18] M. Block, Y. Bao, S. Choi, E. Altman, and N. Y. Yao, *Phys. Rev. Lett.* **128**, 010604 (2022).
- [19] H. Liu, T. Zhou, and X. Chen, *Phys. Rev. B* **106**, 144311 (2022).
- [20] J. Richter, O. Lunt, and A. Pal, *Phys. Rev. Res.* **5**, L012031 (2023).
- [21] P. Sierant, M. Schirò, M. Lewenstein, and X. Turkeshi, *Phys. Rev. Lett.* **131**, 230403 (2023).
- [22] R. Suzuki, J. Haferkamp, J. Eisert, and P. Faist, [arXiv:2305.15475](https://arxiv.org/abs/2305.15475).
- [23] A. Kumar, K. Aziz, A. Chakraborty, A. W. W. Ludwig, S. Gopalakrishnan, J. H. Pixley, and R. Vasseur, *Phys. Rev. B* **109**, 014303 (2024).
- [24] A. Lavasani, Y. Alavirad, and M. Barkeshli, *Nat. Phys.* **17**, 342 (2021).
- [25] K. Klocke and M. Buchhold, *Phys. Rev. B* **106**, 104307 (2022).
- [26] Y. Kuno and I. Ichinose, *Phys. Rev. B* **107**, 224305 (2023).
- [27] A. Lavasani, Y. Alavirad, and M. Barkeshli, *Phys. Rev. Lett.* **127**, 235701 (2021).
- [28] A.-R. Negari, S. Sahu, and T. H. Hsieh, *Phys. Rev. B* **109**, 125148 (2024).
- [29] Y. Kuno, T. Orito, and I. Ichinose, *Phys. Rev. B* **109**, 054432 (2024).
- [30] M. Ippoliti, M. J. Gullans, S. Gopalakrishnan, D. A. Huse, and V. Khemani, *Phys. Rev. X* **11**, 011030 (2021).
- [31] A. Sriram, T. Rakovszky, V. Khemani, and M. Ippoliti, *Phys. Rev. B* **108**, 094304 (2023).
- [32] Y. Kuno, T. Orito, and I. Ichinose, *Phys. Rev. B* **108**, 094104 (2023).
- [33] A. Lavasani, Z. X. Luo, and S. Vijay, *Phys. Rev. B* **108**, 115135 (2023).
- [34] G.-Y. Zhu, N. Tantivasadakarn, and S. Trebst, [arXiv:2303.17627](https://arxiv.org/abs/2303.17627).
- [35] R. Raussendorf and H. J. Briegel, *Phys. Rev. Lett.* **86**, 5188 (2001).
- [36] R. Raussendorf, J. Harrington, and K. Goyal, *Ann. Phys.* **321**, 2242 (2006).
- [37] H. J. Briegel, D. E. Browne, W. Dür, R. Raussendorf, and M. Van den Nest, *Nat. Phys.* **5**, 19 (2009).
- [38] T.-C. Wei, *Adv. Phys.* **3**, 1461026 (2018).
- [39] R. Verresen, N. Tantivasadakarn, and A. Vishwanath, [arXiv:2112.03061](https://arxiv.org/abs/2112.03061).
- [40] N. Tantivasadakarn, R. Thorngren, A. Vishwanath, and R. Verresen, *Phys. Rev. X* **14**, 021040 (2024).
- [41] J. Y. Lee, W. Ji, Z. Bi, and M. P. A. Fisher, [arXiv:2208.11699](https://arxiv.org/abs/2208.11699).
- [42] T.-C. Lu, Z. Zhang, S. Vijay, and T. H. Hsieh, *PRX Quantum* **4**, 030318 (2023).
- [43] R. Raussendorf, S. Bravyi, and J. Harrington, *Phys. Rev. A* **71**, 062313 (2005).
- [44] I. Angelidi, M. Szyniszewski, and A. Pal, [arXiv:2306.13008](https://arxiv.org/abs/2306.13008).
- [45] E. H. Chen, G.-Y. Zhu, R. Verresen, A. Seif, E. Baumer, D. Layden, N. Tantivasadakarn, G. Zhu, S. Sheldon, A. Vishwanath, S. Trebst, and A. Kandala, [arXiv:2309.02863](https://arxiv.org/abs/2309.02863).
- [46] D. Gottesman, [arXiv:quant-ph/9807006](https://arxiv.org/abs/quant-ph/9807006).
- [47] S. Aaronson and D. Gottesman, *Phys. Rev. A* **70**, 052328 (2004).
- [48] M. Suzuki, *Prog. Theor. Phys.* **46**, 1337 (1971).
- [49] S. O. Skrvøseth and S. D. Bartlett, *Phys. Rev. A* **80**, 022316 (2009).
- [50] P. Smacchia, L. Amico, P. Facchi, R. Fazio, G. Florio, S. Pascazio, and V. Vedral, *Phys. Rev. A* **84**, 022304 (2011).
- [51] S. M. Giampaolo and B. C. Hiesmayr, *Phys. Rev. A* **92**, 012306 (2015).
- [52] V. Lahtinen and E. Ardonne, *Phys. Rev. Lett.* **115**, 237203 (2015).
- [53] R. Morral-Yepes, F. Pollmann, and I. Lovas, *Phys. Rev. B* **108**, 224304 (2023).
- [54] W. Son, L. Amico, R. Fazio, A. Hamma, S. Pascazio, and V. Vedral, *Europhys. Lett.* **95**, 50001 (2011).
- [55] R. Verresen, R. Moessner, and F. Pollmann, *Phys. Rev. B* **96**, 165124 (2017).
- [56] N. Tantivasadakarn, R. Thorngren, A. Vishwanath, and R. Verresen, *SciPost Phys.* **14**, 012 (2023).
- [57] M. A. Nielsen and I. L. Chuang, *Quantum Computation and Quantum Information* (Cambridge University Press, Cambridge, 2010).
- [58] D. Fattal, T. S. Cubitt, Y. Yamamoto, S. Bravyi, and I. L. Chuang, [arXiv:quant-ph/0406168](https://arxiv.org/abs/quant-ph/0406168).
- [59] A. Nahum, J. Ruhman, S. Vijay, and J. Haah, *Phys. Rev. X* **7**, 031016 (2017).
- [60] N. Lang and H. P. Büchler, *Phys. Rev. B* **102**, 094204 (2020).
- [61] C. Fechisin, N. Tantivasadakarn, and V. V. Albert, [arXiv:2312.09272](https://arxiv.org/abs/2312.09272).
- [62] T. C. Lu, L. A. Lessa, I. H. Kim, and T. H. Hsieh, *PRX Quantum* **3**, 040337 (2022).
- [63] S. Seifnashri and S.-H. Shao, [arXiv:2404.01369](https://arxiv.org/abs/2404.01369).